Investigation of Low-Energy Event Detection through Meissner Screening probed by a Superconductor–NV Center ensemble

J. Bogenschuetz, P. Sau, B. Brown, Y. Mei, J. Asaadi, V. A. Chirayath
Department of Physics, University of Texas at Arlington – 76019

CPAD 2025, Oct 7 – 10, 2025, Inn at Penn, University of Pennsylvania

(on behalf of P. Sau)

Outline

- Concept of the Superconductor-NV center detector.
- Simulations on the working principle of the detector.
- Can the NV center probing laser destroy superconducting properties?
- Rare particle searches using the superconductor-NV center ensemble.
- NV center research at UTA.
- Summary and Future directions.

Superconductor-NV center Ensemble

- Structure
  - Superconducting thing film (Aluminum with T_c ~ 1.1 K)
  - Diamond thin-film with NV centers
  - DC magnetic field ~ 1mT
- Meissner Screening
  - Reduce field at the NV center
- Transition of the superconductor to normal state results in a change of field intensity at the NV center.

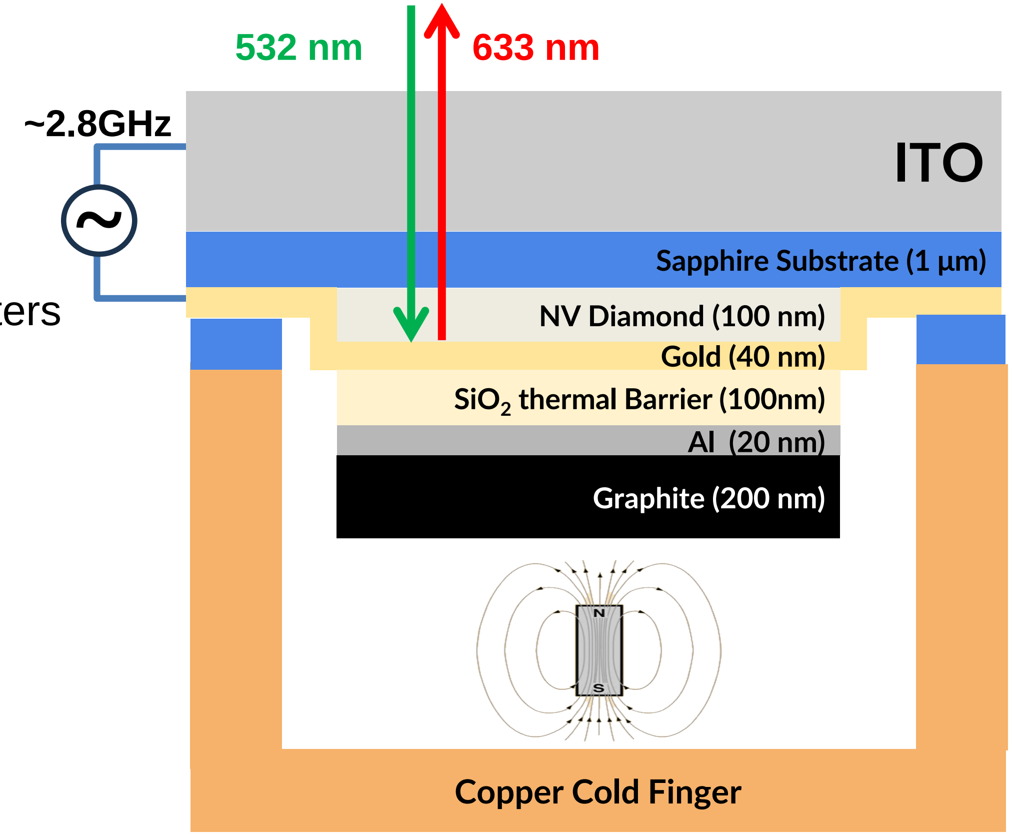

J. Bogenschuetz, B. Brown et al. (manuscript under preparation)

Meissner Effect

- Above the transition temperature T_c applied magnetic field (B_a) permeates the metallic cylinder.
- Below T_c the superconductor spontaneously excludes the magnetic field.

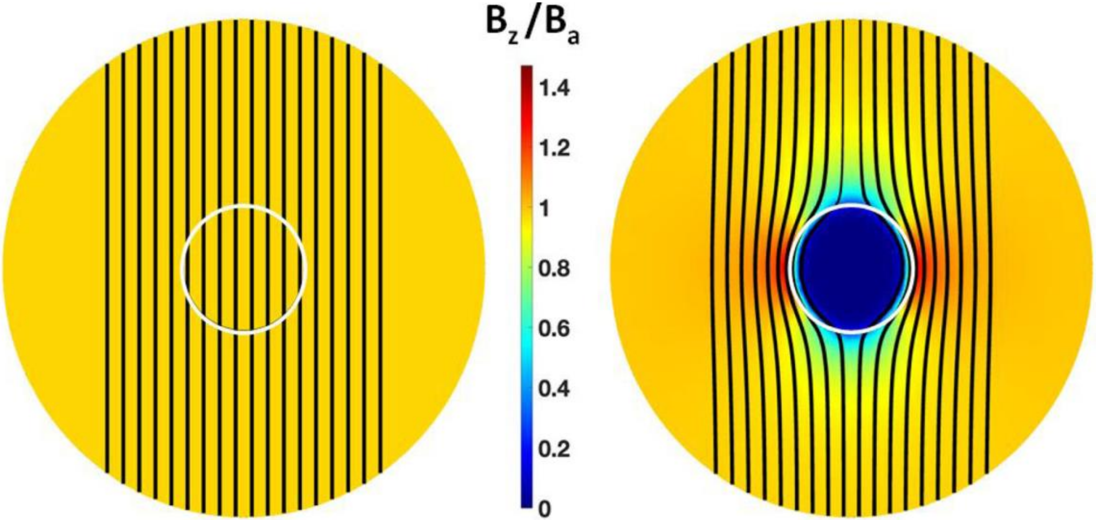

S. M. Anlage, IEEE Journal of Microwaves, Vol.1, No.1, 389-402

Meissner Effect

- At the operating temperature (1.085 K) the field at the NV center is only about 75% of the applied field.
- For an applied field of 1mT, there will be a variation of 250 µT as the superconductor transitions to the normal state.

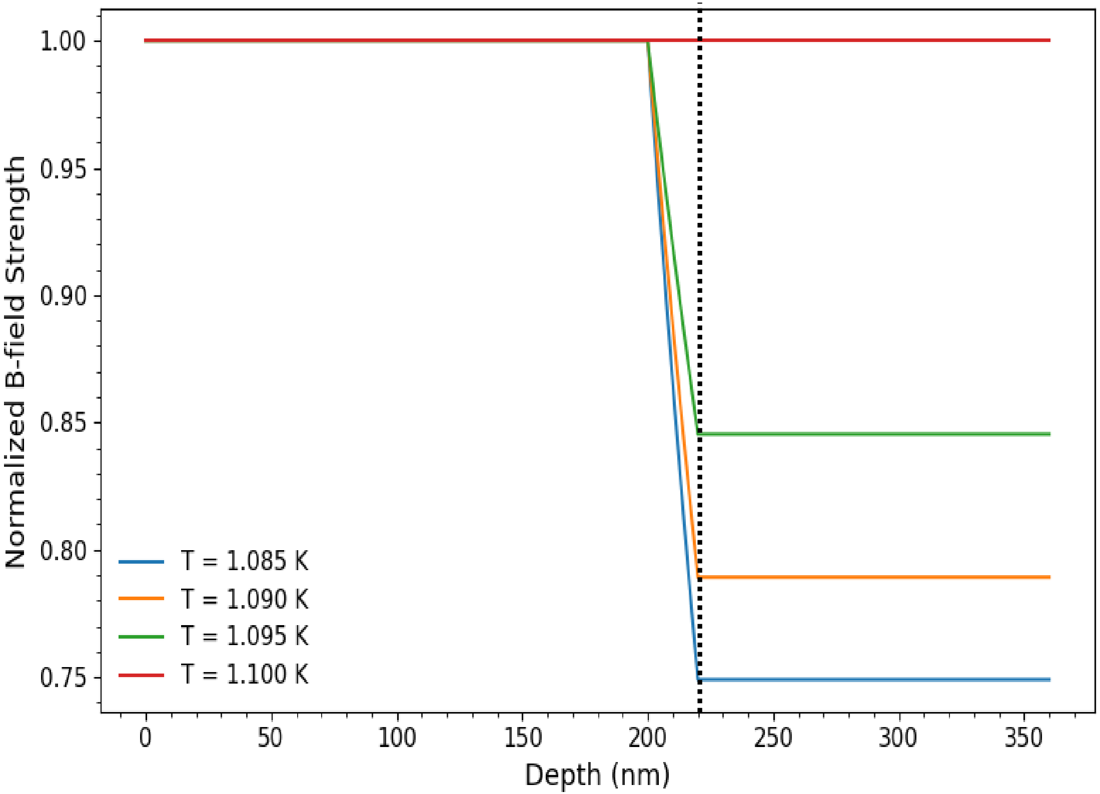

J. Bogenschuetz, B. Brown et al. (manuscript under preparation)

Nitrogen Vacancy (NV) centers in diamond

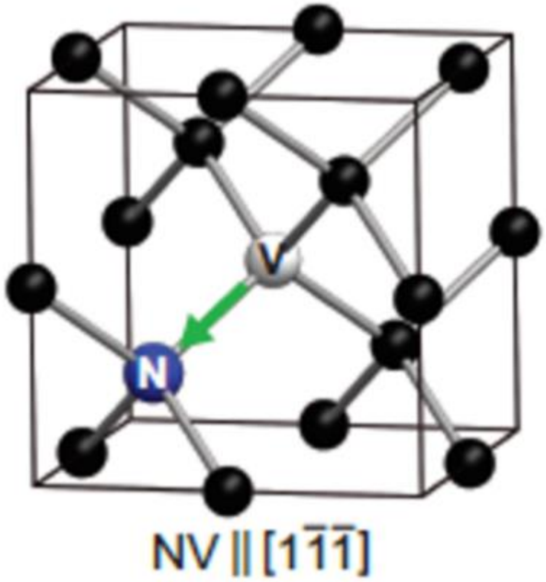

The NV center in a diamond unit cell.

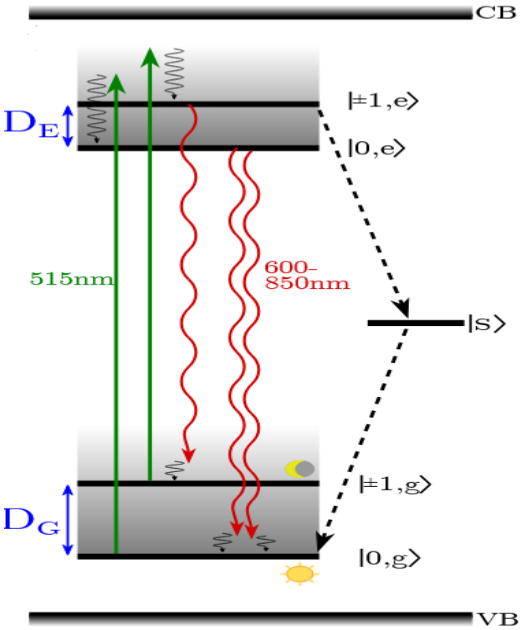

Simplified energy diagram of the NV center defect which lie in the 5.5 eV bandgap of diamond.

Fundamentals of magnetic field measurement with NV centers in diamond (Qnami Technical Note)

Nitrogen Vacancy (NV) centers in diamond

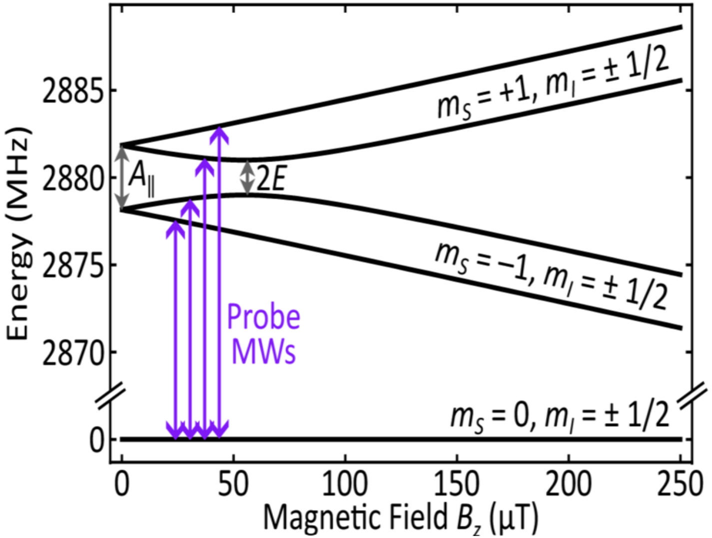

NV ground state energy levels as a function of on-axis field

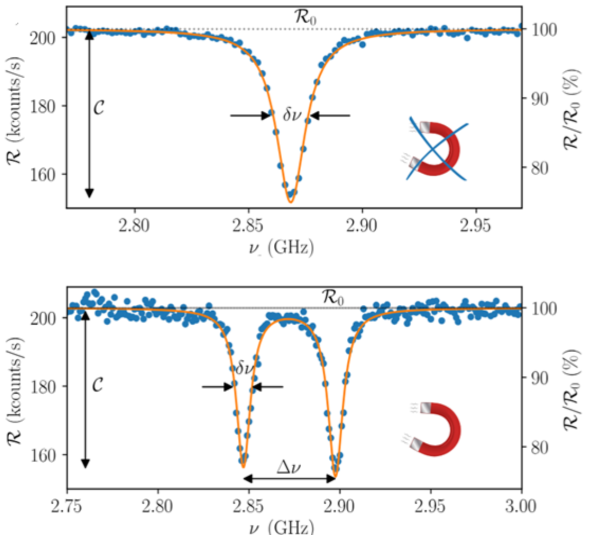

Top Panel: Fluorescence spectra NV center with no applied magnetic field. Bottom panel: Fluorescence spectra revealing Zeeman splitting with an applied on-axis field of 1 mT.

R.T. Kapur et al., arXiv:2506.01906v1
Fundamentals of magnetic field measurement with NV centers in diamond (Qnami Technical Note)

Simulated fluorescence spectra of NV center

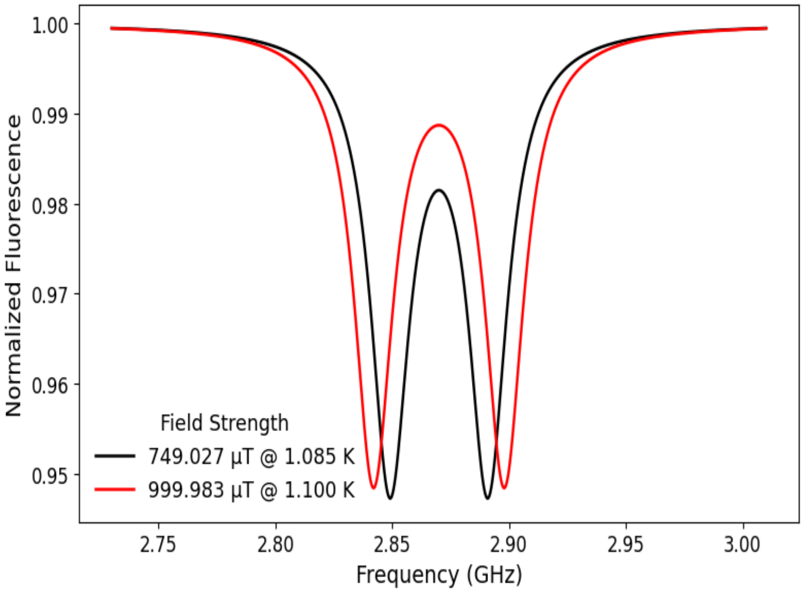

Calculated ODMR spectra for NV centers assuming 5% contrast and 100 kHz line width as a function of on-axis field

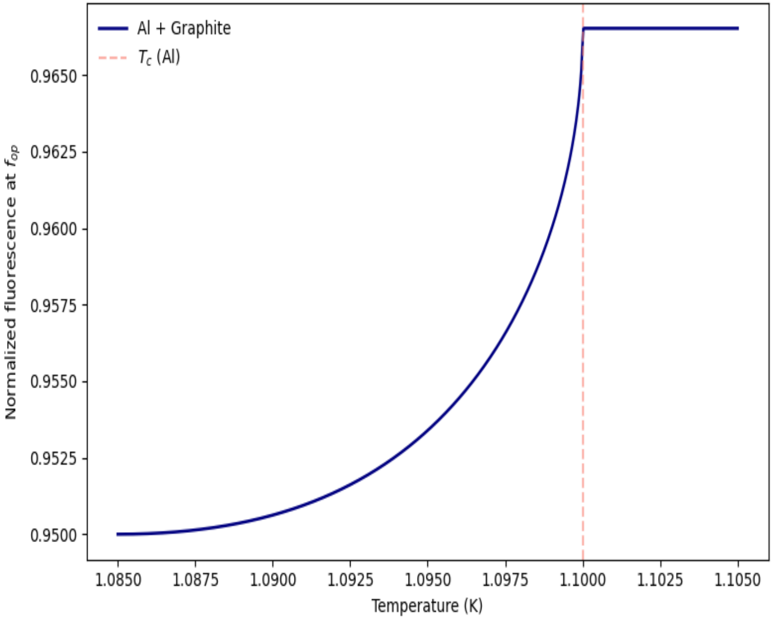

Increase in the fluorescence intensity as the temperature of the superconductor increases from operating temperature to T_c.

J. Bogenschuetz, B. Brown et al. (manuscript under preparation)

Simulated fluorescence spectra of NV center

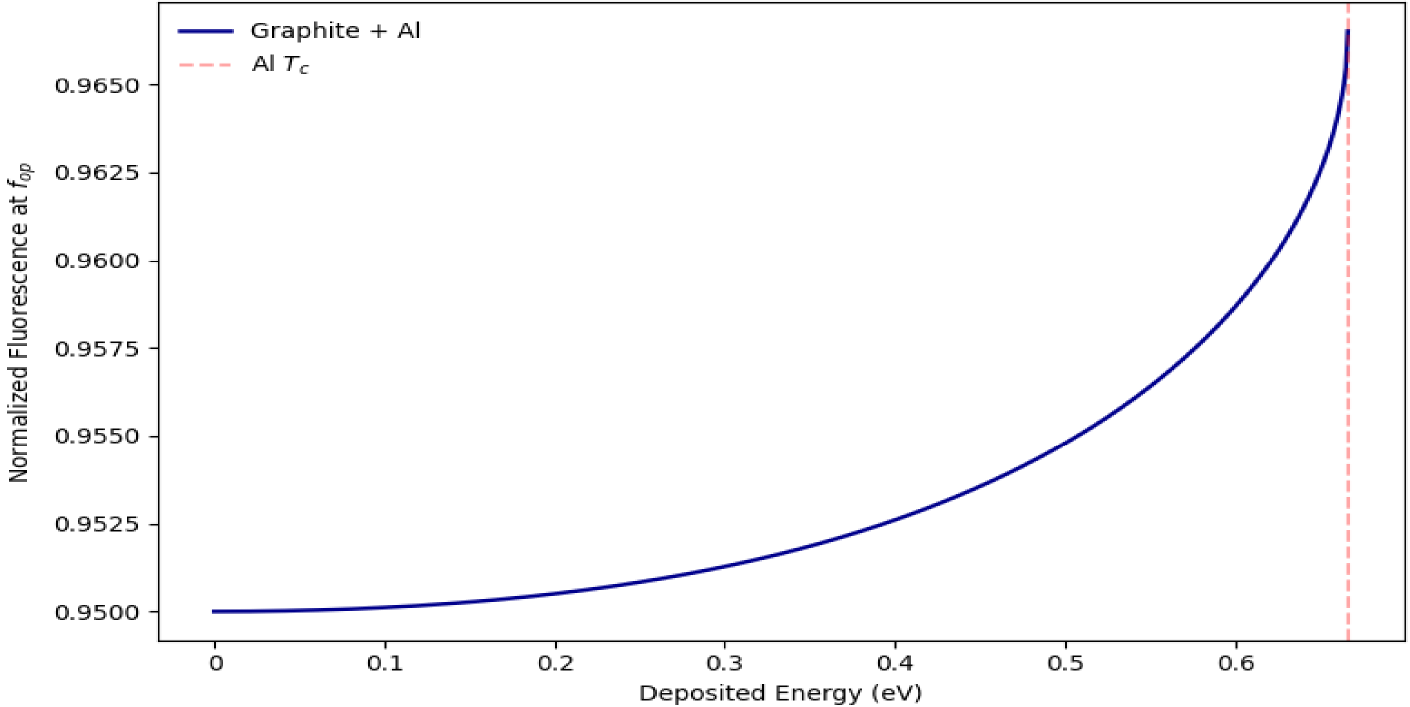

Energy deposited versus the change in fluorescence intensity after considering the magnetic field variation at the NV center. .

J. Bogenschuetz, B. Brown et al. (manuscript under preparation)

Simulated fluorescence spectra of NV center

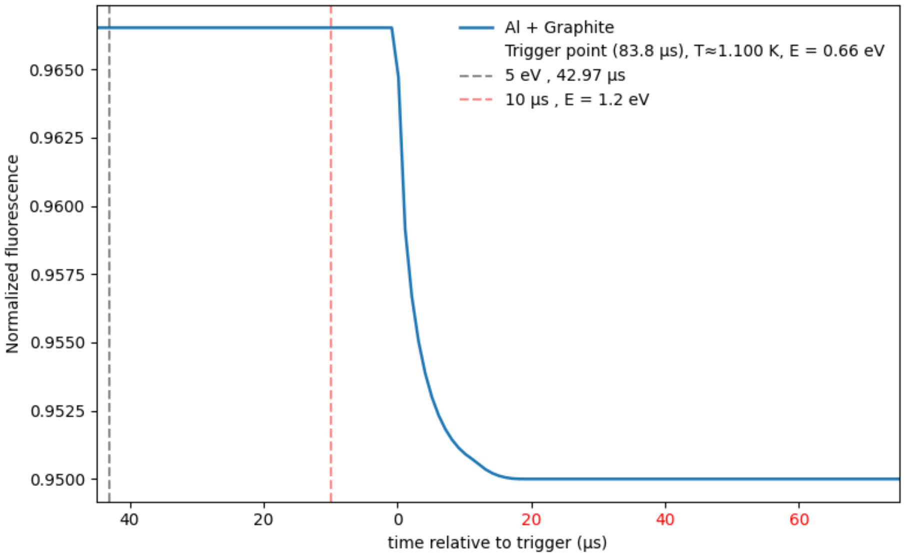

Time for which the fluorescence intensity stays high before dropping down to the intensity at operating temperature.

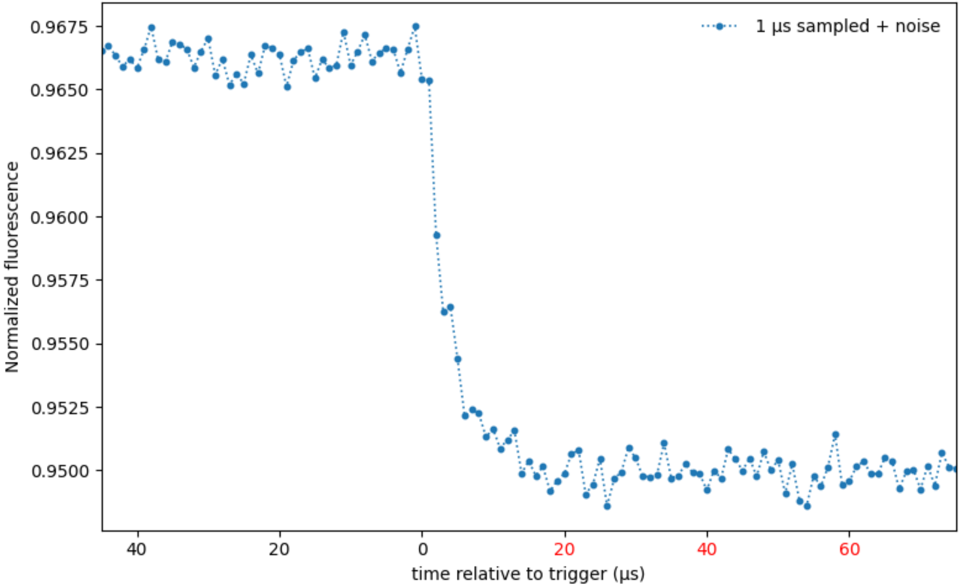

Time for which the fluorescence intensity stays high before dropping down to the intensity at operating temperature. Here we have included synthetic noise taken from R.T. Kapur et al., (arXiv:2506.01906v1) which had a similar NV center setup.

J. Bogenschuetz, B. Brown et al. (manuscript under preparation)

Can the NV center probing laser destroy superconducting properties?

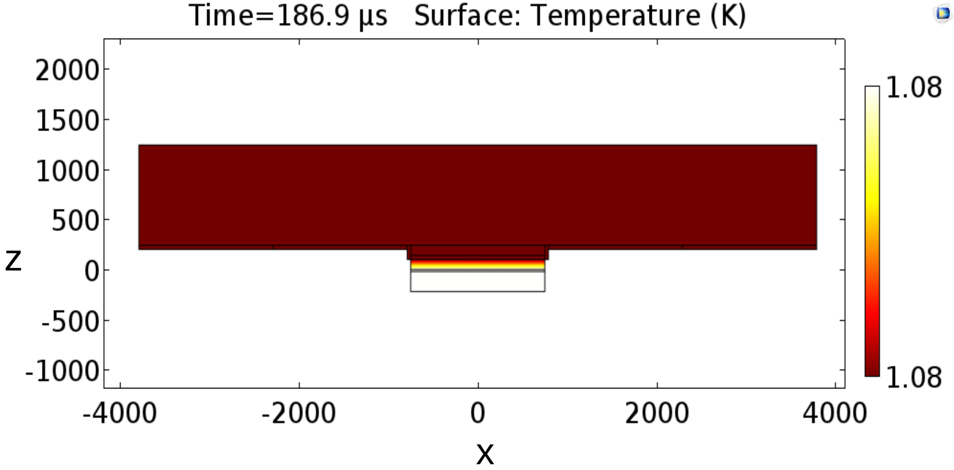

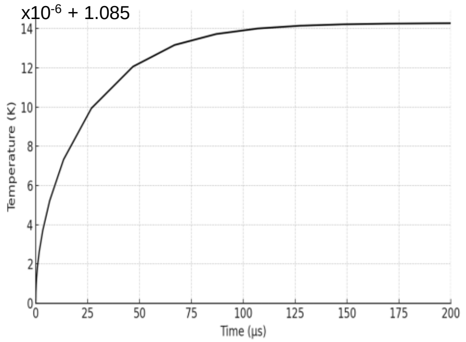

Time required for the temperature of the Al sensor to stabilize after the laser is turned on

COMSOL simulation which combines optical module with thermodynamic module. Here we have considered a laser power input of 15mW/mm^2. The temperature profile across different layers is shown on the right by taking a cut at x=0

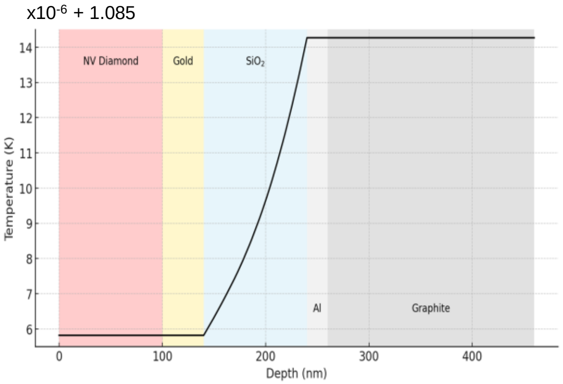

J. Bogenschuetz, B. Brown et al. (manuscript under preparation)

Rare particle searches using NV center-Superconductor ensemble?

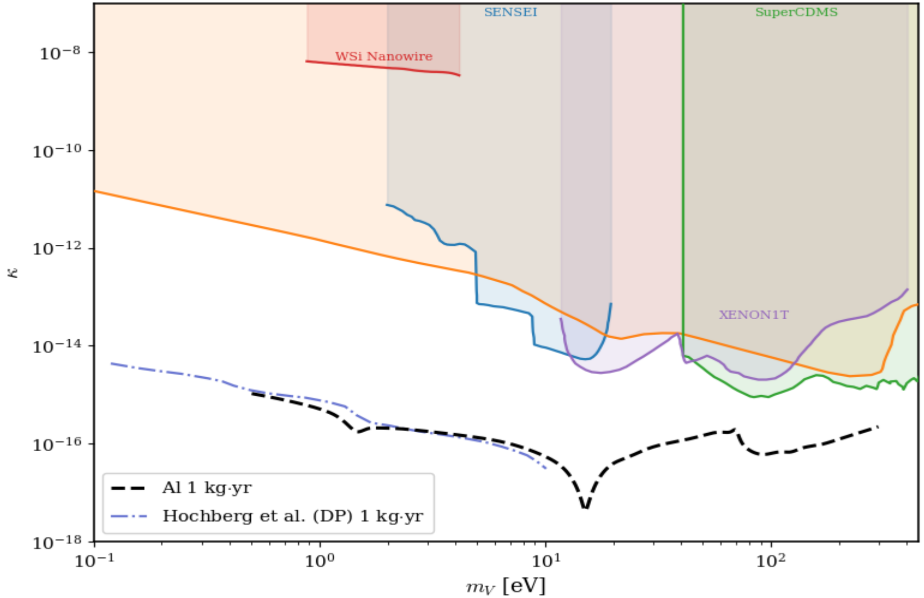

Estimated sensitivity of an aluminum superconductor target for 1-kg-year (dash-dot blue line from Hochberg et al) and dotted line for this work.

J. Bogenschuetz, B. Brown et al. (manuscript under preparation)
Hochberg et al , "Detecting Ultralight Bosonic Dark Matter via Absorption in Superconductors", . arXiv:1604.06800

Rare particle searches using NV center-Superconductor ensemble?

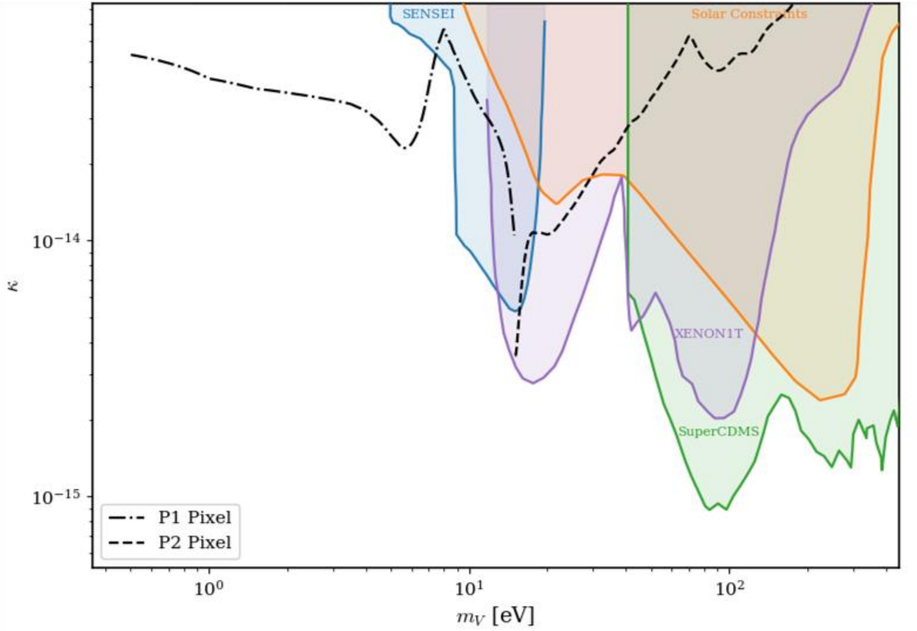

Estimated sensitivity of our aluminum + graphite pixel covering a 10 cm^2 area with 50% coverage.

J. Bogenschuetz, B. Brown et al. (manuscript under preparation)

NV Center based research at UTA

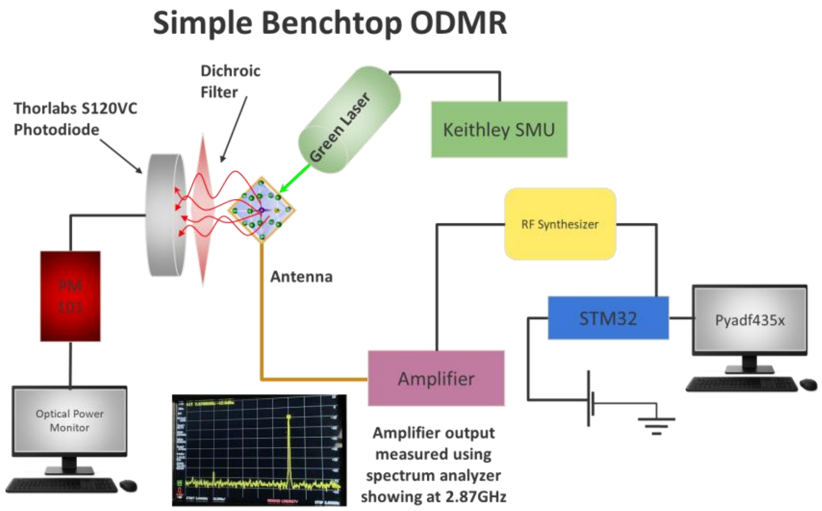

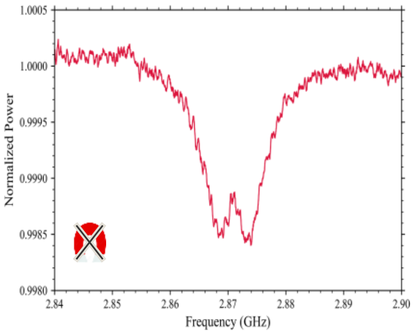

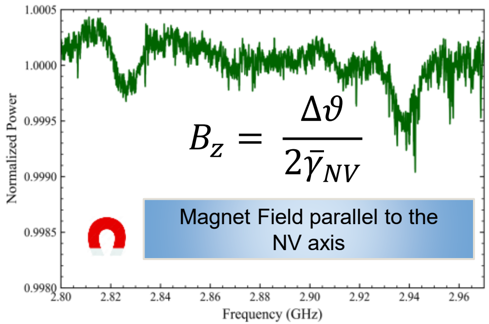

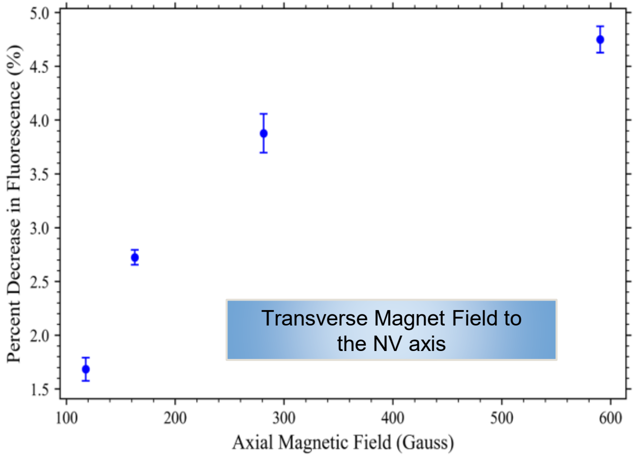

P. Sau et al. (manuscript under preparation)

NV Center based research at UTA

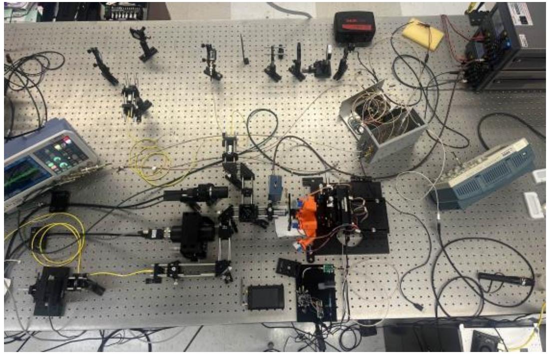

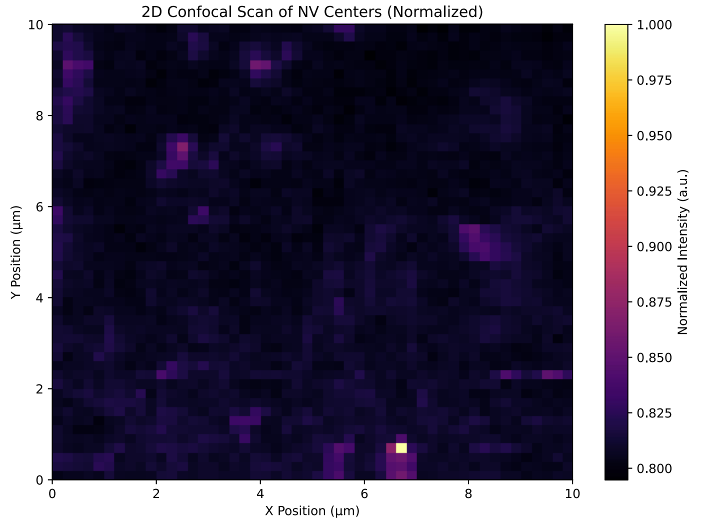

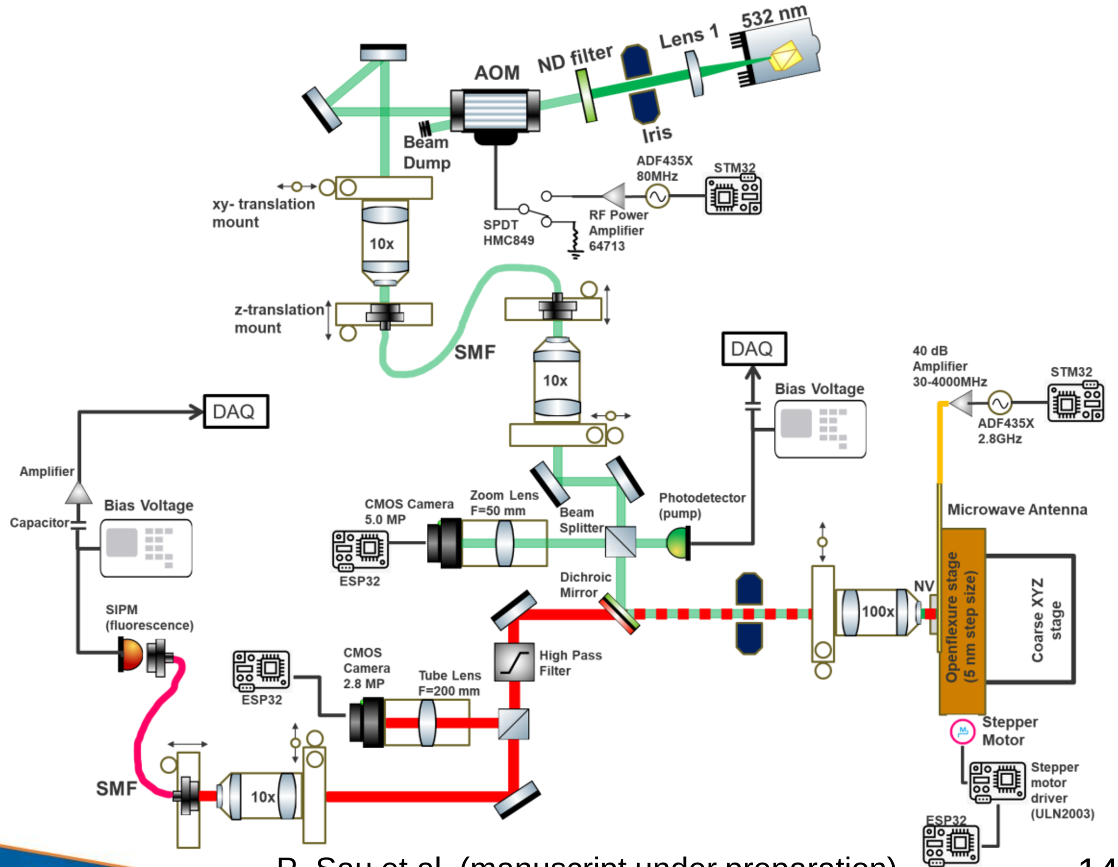

P. Sau et al. (manuscript under preparation)

Future Directions

Multipixel Superconductor-NV center detector

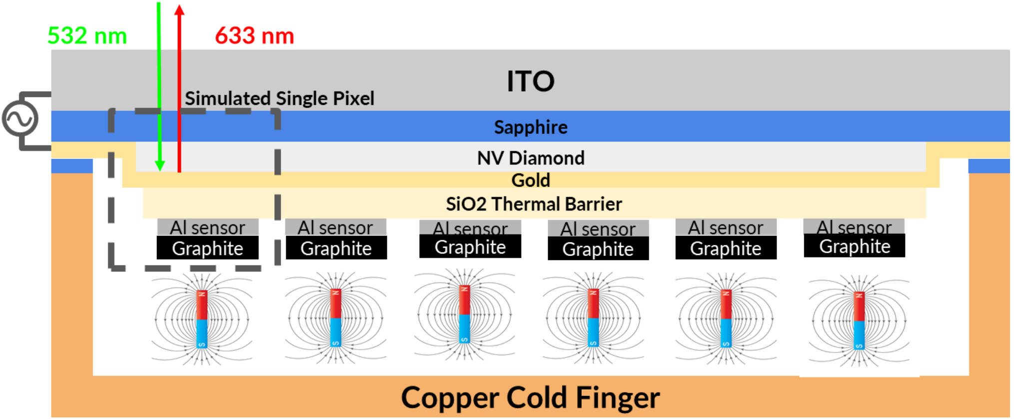

- Demonstrate the operation of single pixel using an optical cryostat with an alpha source.
- We are presently working on a design which will couple our table top NV center system to the optical cryostat.

J. Bogenschuetz et al. (manuscript under preparation)

Summary

- We have presented a novel detector which combines Meissner screening of superconductor and NV center based magnetometry.
- Initial COMSOL based Multiphysics simulations have shown that with proper choice of superconductor we are competitive for Dark photon absorption in the energy range of 1 – 10 eV.
- We have developed the required expertise at UTA to facilitate the demonstration of our single pixel detector.

Thanks

Material	Index of Refraction (APS short)	Index DOI	Thermal Conductivity (APS short)	Thermal DOI	Specific Heat (APS short)	Specific DOI	London Penetration Depth (APS short)	London DOI
Diamond	Philipp & Taft, Phys. Rev. 136, A1445 (1964).	10.1103/PhysRev.136.A1445	Berman, Simon & Ziman, Proc. R. Soc. A 220, 171 (1953).	10.1098/rspa.1953.0180	Burn & Friedberg, Phys. Rev. 111, 1275 (1958).	10.1103/PhysRev.111.1275		
Gold (Au)	Hagemann, Gudat & Kunz, DESY Rep. SR-74/7 (1974); Johnson & Christy, Phys. Rev. B 6, 4370 (1972).	10.1103/PhysRevB.6.4370	Rosenberg, Philos. Trans. R. Soc. A 247, 441 (1955).	10.1098/rsta.1955.0003	Martin, Phys. Rev. 170, 650 (1968).	10.1103/PhysRev.170.650		
SiO2 (Silica)	Rodríguez-de Marcos et al., Opt. Mater. Express 6, 3622 (2016).	10.1364/OME.6.003622	Zeller & Pohl, Phys. Rev. B 4, 2029 (1971).	10.1103/PhysRevB.4.2029	Zeller & Pohl, Phys. Rev. B 4, 2029 (1971).	10.1103/PhysRevB.4.2029		
Aluminum (Al)	See Gold		Andrews, Webber & Spohr, Phys. Rev. 84, 994 (1951).	10.1103/PhysRev.84.994	Phillips, Phys. Rev. 114, 676 (1959); Caplan & Chanin, Phys. Rev. 138, A1428 (1965).	10.1103/PhysRev.114.676; 10.1103/PhysRev.138.A1428	Faber & Pippard, Proc. R. Soc. A 231, 336 (1955); Behroozi et al., Phys. Rev. B 10, 2756 (1974).	10.1098/rspa.1955.0178; 10.1103/PhysRevB.10.2756
Graphite	See Al	10.1103/PhysRev.138.A197	Morelli & Uher, Phys. Rev. B 31, 6721 (1985).	10.1103/PhysRevB.31.6721	Keesom & Pearlman, Phys. Rev. 99, 1119 (1955).	10.1103/PhysRev.99.1119		
Germanium (Ge)	Ciesielski et al., Mater. Sci. Semicond. Process. 81, 64 (2018); Amotchkina et al., Appl. Opt. 59, A40 (2020).	10.1016/j.mssp.2018.03.003; 10.1364/AO.59.000A40	Asen-Palmer et al., Phys. Rev. B 56, 9431 (1997).	10.1103/PhysRevB.56.9431	Keesom & Seidel, Phys. Rev. 113, 33 (1959).	10.1103/PhysRev.113.33		
Silicon (Si)	See Germanium		White & Woods, Phys. Rev. 103, 569 (1956); Glassbrenner & Slack, Phys. Rev. 134, A1058 (1964).	10.1103/PhysRev.103.569; 10.1103/PhysRev.134.A1058	Keesom & Seidel, Phys. Rev. 113, 33 (1959).	10.1103/PhysRev.113.33		
Tungsten (W)	Werner, Glantschnig & Ambrosch-Draxl, J. Phys. Chem. Ref. Data 38, 1013 (2009); Windt et al., Appl. Opt. 27, 246 (1988).	10.1063/1.3243762; 10.1364/AO.27.000246	Wagner, Garland & Bowers, Phys. Rev. B 3, 3141 (1971).	10.1103/PhysRevB.3.3141	Black, Phys. Rev. Lett. 21, 28 (1968).	10.1103/PhysRevLett.21.28		
Niobium Nitride (NbN)	Paul, Zhou & Berggren, arXiv 2503.00169v2 (2025); RD39 Collaboration, CERN-EP/99-54 (1999).	10.48550/arXiv.2503.00169	RD39 Collaboration, Superconducting NbN Microstrip Detectors, CERN-EP/99-54 (1999).		Geballe et al., Physics 2, 293 (1966).		Kamlapure et al., Appl. Phys. Lett. 96, 072509 (2010); Shapoval et al., Phys. Rev. B 83, 214517 (2011).	10.1063/1.3314308; 10.1103/PhysRevB.83.214517

Energy Loss Function Calculation

Consider a hidden photon which is kinetically mixed with the hypercharge gauge boson, leading to kinetic mixing with the photon,

$$\mathcal{L} \supset -\frac{\kappa}{2} F_{\mu\nu} V^{\mu\nu}\,, \tag{18}$$

Find *n* and *k* data, calculate Re[ε], Im[ε] (Eq 1.)

↓

Calculate ELF from data (Eq. 2)

↓

Fit ELF using many Drude-Lindhard oscillators (Eq. 3)

↓

Check *f*-sum and *p*-sum (Eq. 4-5) and error relative to data

↓

ELF(ω, *q*=0)

Data was pulled from refractiveindex.info Hagemann et al. for both Al and Thin-Amorphous C
Eq. 1-2 by definition, Eq. 3 - 5 are from Sun et al theory section

$$\varepsilon_1(\omega) = n(\omega)^2 - k(\omega)^2, \tag{1a}$$

$$\varepsilon_2(\omega) = 2\,n(\omega)\,k(\omega). \tag{1b}$$

$$\mathrm{ELF}(\omega) = \Im\left(-\frac{1}{\varepsilon(\omega)}\right) = \frac{\varepsilon_2(\omega)}{\varepsilon_1(\omega)^2 + \varepsilon_2(\omega)^2} = \frac{2\,n(\omega)\,k(\omega)}{\left[n(\omega)^2 - k(\omega)^2\right]^2 + \left[2\,n(\omega)\,k(\omega)\right]^2}. \tag{2}$$

$$\mathrm{ELF}(\omega) \;=\; \sum_{j=1}^{N_{\mathrm{osc}}} a_j \frac{\omega_{p,j}^2\,\gamma_j\,\omega}{\left(\omega^2 - \omega_{p,j}^2\right)^2 + (\gamma_j\,\omega)^2}. \tag{3}$$

$$Z_{\mathrm{eff}} = \frac{2}{\pi\,\Omega_{p,1}^2}\int_0^\infty \omega\,\mathrm{ELF}(\omega)\,d\omega \;\approx\; Z_{\mathrm{ref}}. \tag{4}$$

$$P_{\mathrm{eff}} = \frac{2}{\pi}\int_0^\infty \frac{\mathrm{ELF}(\omega)}{\omega}\,d\omega \;\approx\; 1. \tag{5}$$

https://drive.google.com/drive/folders/16kY0DK22JIi5Twz4g7WC8l5U2i0wA_Vq?usp=sharing

Fit Code Breakdown

Import data, interpolate between points, calculate ELF

Seed poles: use peak finding to get initial

Stage A: Fit to data with linear residuals (no constraints).

Merge poles: combine near-duplicate oscillators.

Stage B: Enforce:

- f-sum rule
- p-sum rule
- UV tail slope →ωe-3

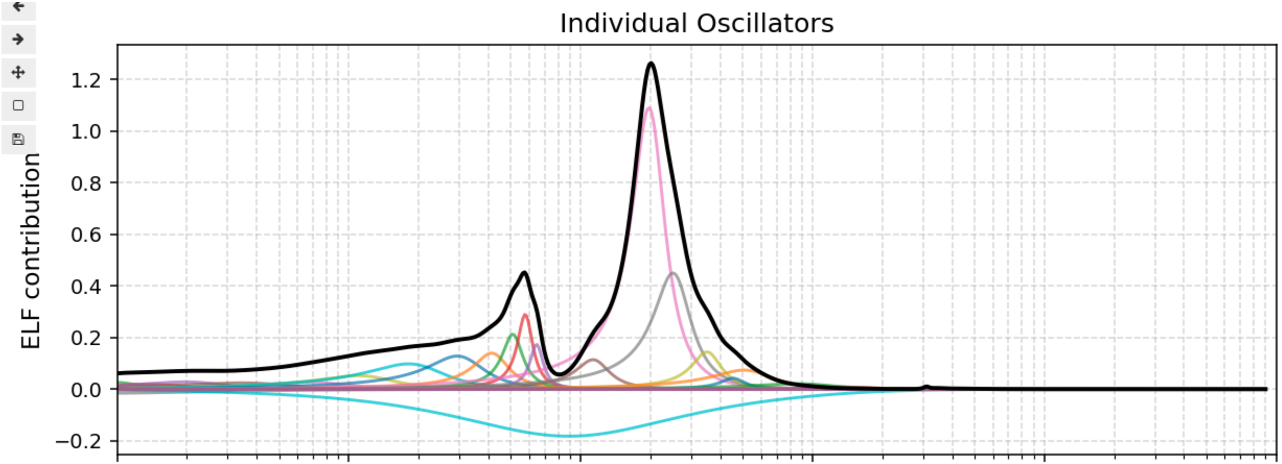

Fits for Aluminum and Graphite

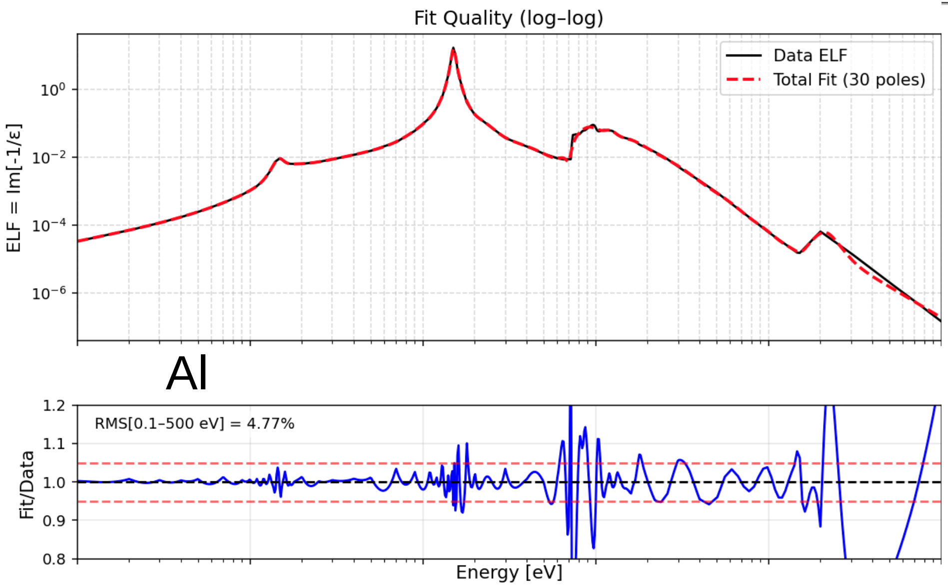

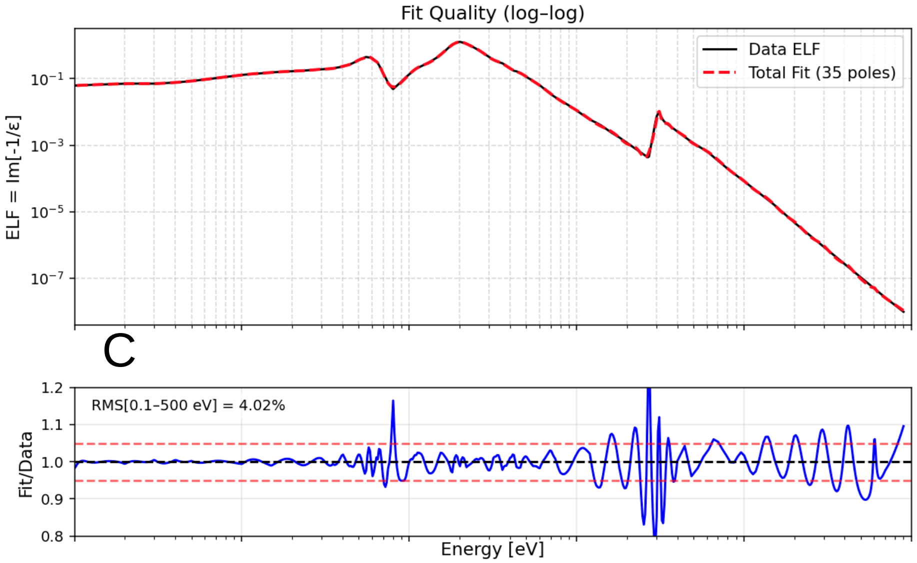

Dark Photon Absorption

$$R_V(\kappa, m_V) = \frac{\rho_X}{\rho_T}\,\kappa^2\,\mathrm{ELF}(m_V),$$

$$N_{\mathrm{events}}(\kappa, m_V) = R_V(\kappa, m_V)\ \times \mathrm{exposure},$$

$$N_{\mathrm{target}} \leq N_{\mathrm{events}}(\kappa, m_V),$$

$$\kappa(m_V) = \sqrt{\frac{N_{\mathrm{target}}}{\mathrm{exposure}\ \cdot\ \frac{\rho_X}{\rho_T}\,\mathrm{ELF}(m_V)}}$$

$$\frac{\rho_X}{\rho_T}$$

DM density, 0.4 GeV/cm^3

Target density, g/cm^3

3 events for 95% CL

Minimum Kinetic Mixing to achieve target events as a function of DM mass

Grams X year

DM Mass

Particle detection using NV-Centers

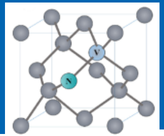

- NV centers have been utilized for imaging Mei
  effect and Flux vortices in superconductors [1,2]

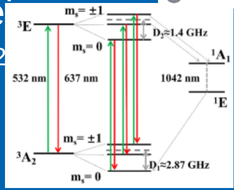

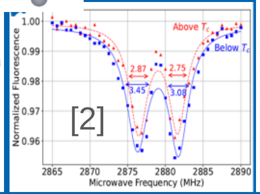

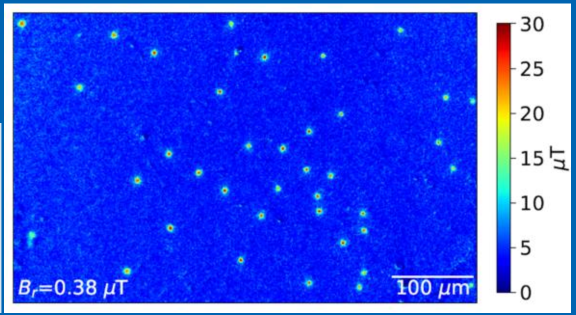

Blue-Sky idea: **Use NV center magnetometry to probe Meissner exclusion as the superconductor transitions to normal state due to energy deposition by a particle (Dark Matter) of interest!**

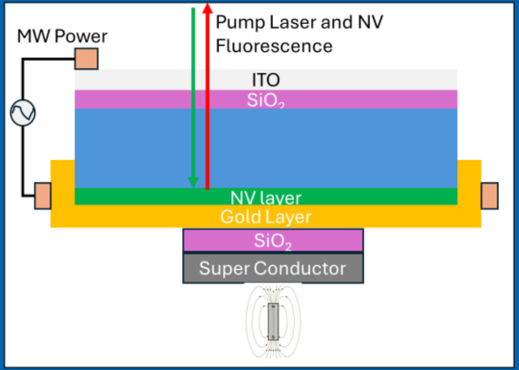

- The super conductor is maintained close to its transition temperature (example 1.1K for Al).
- Particle of certain energy (~100eV) takes the superconductor to above its transition temperature (say 1.6 K), the magnetic field reaches the NV center and changes the fluorescence spectra (see example figure from [1] which shows the resonance frequency shifts with the transition).
- Measure fluorescence intensity [3], width of the ODMR spectra (see [2]) or resonance frequency to detect the presence of energy deposition.

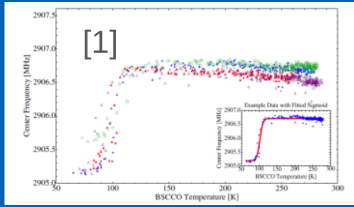

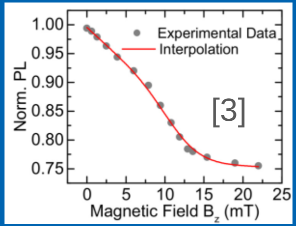

1. Louis-S Bouchard et al., “Detection of the Meissner effect with a diamond Magnetometer”, 2011, New J. Phys. 13 025017
2. R.T. Kapur et al., “Flux Trapping Characterization for Superconducting Electronics Using a Cryogenic Widefield NV-Diamond Microscope”, 2025, https://arxiv.org/abs/2506.01906
3. D. Paone et al., “All-optical and microwave-free detection of Meissner screening using nitrogen-vacancy centers in diamond”, 2021, J. Appl. Phys. 129, 024306;; doi: 10.1063/5.0037414

Preliminary simulation results of NV-Center based Meissner exclusion imaging

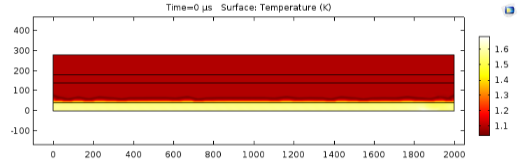

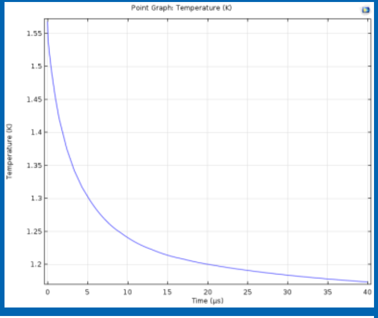

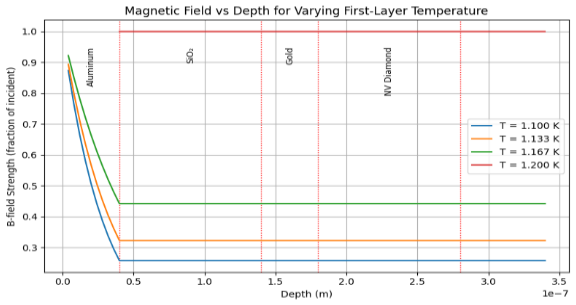

Comsol simulation of the 4 layers taken from the conceptual design. This is at time t=0, with the temperature of superconductor increased to > 1.6 K.

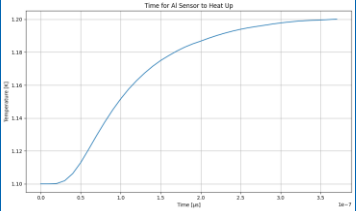

Time taken by the superconductor to come back to operating temperature below its Tc. If we read NV center for 10 us - it allows us to measure changes as small as ~ 10 uT (assuming that we can reach the easily achievable 32 nT/√Hz) [4].

As the superconductor transition to normal state, magnetic field at NV center increases from ~ 250 uT to 1 mT.

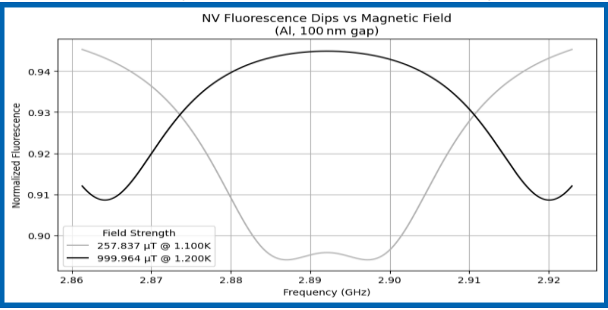

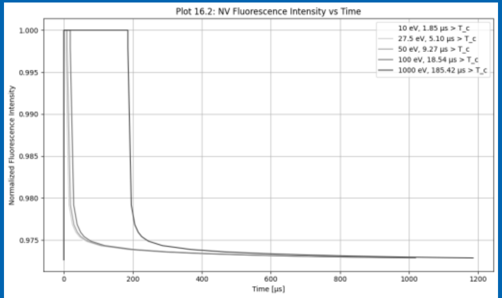

Side Note: A 2umx2um superconductor takes only 100s of femtosecond to come to equilibrium. However even considering that phonon transport is less than microseconds.

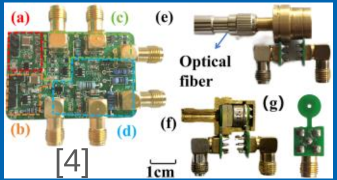

For field just below the critical field of the superconductor (eg., 1mT for Al), the change in magnetic field at NV center is ~ 750 uT.

In terms of energy, we are looking at ~ 100 eV energy deposition.(non thermal sterile neutrino like DM candidates).

4. Qin Hu et al., “Design of high sensitivity magnetometer based on Diamond Nitrogen-Vacancy Centers and Weak Signal Output Module”, (2025) Diamond & Related Materials 151, 111858.

Potential Applications and advantages of NV-Center based magnetometry coupled with superconductors

Advantages: NV center based optical read out provides a scalable, electromagnetic interference free data transfer from low temperature (~mK) to room temperature for technologies that employ superconductors. (see other efforts for a full photonic read out here[5]).

Dark Matter searches: Recent investigations have shown that superconductors can probe dark matter with possibility of obtaining directionality [6].

Dark Matter searches: NV center themself can be used for dark matter searches. Readout and on chip integration developed will be useful for these efforts [7].

Broader impact: Miniaturized NV center detectors coupled to a fiber-microwave antenna coupled: Mapping precise magnetic fields in atomic beam [8] (eg. neutrino mass measurement in Project 8 requires precise mapping of the magnetic field in the Tritium trap)

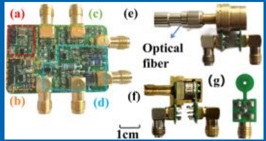

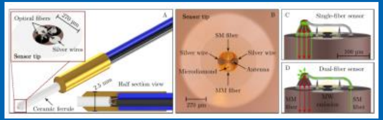

5. Marc de Cea et al., “Photonic Readout of Superconducting Nanowire Single Photon Counting Detectors”, 2020, Scientific Reports, 10:9470.
6. Y. Hochberg et al., “Directional detection of light dark matter in superconductors”, 2023, Phys. Rev. D. 107, 076015.
7. So Chigusa et al., “Nuclear Spin Metrology with Nitrogen Vacancy Center in Diamond for Axion Dark Matter Detection”, 2025, arXiv:2407.07141v2.
8. S. Johansson et al., “A miniaturized magnetic field sensor based on nitrogen-vacancy centers”, 2025, arXiv:2402.19372v3